

Pressure-Induced Polaronic to Itinerant Electronic Transition in $\text{La}_{1-x}\text{Sr}_x\text{MnO}_3$ Crystals

J.-S. Zhou,¹ J. B. Goodenough,¹ A. Asamitsu,² and Y. Tokura^{2,3}

¹Center for Materials Science & Engineering, ETC 9.102, University of Texas at Austin, Austin, Texas 78712-1063

²Joint Research Center for Atom Technology (JRCAT), Tsukuba 305, Japan

³Department of Applied Physics, University of Tokyo, Tokyo 113, Japan

(Received 8 April 1997)

Measurements of the temperature dependence of the resistivity $\rho(T)$ and thermoelectric power $\alpha(T)$ under several hydrostatic pressures were made on single crystals of $\text{La}_{1-x}\text{Sr}_x\text{MnO}_3$ with $x = 0.12$ and 0.15 in which charge ordering takes place below T_{co} . We report a transition from the polaronic to an itinerant electronic state in the pressure range $5 < P < 6$ kbar in the $x = 0.15$ sample. The polaronic state is modeled as a mobile three-manganese cluster within a matrix of dynamic Jahn-Teller deformations at Mn(III) ions. [S0031-9007(97)04350-0]

PACS numbers: 72.15.Jf, 71.30.+h, 75.30.Kz

In the perovskite system $\text{La}_{1-x}\text{Sr}_x\text{MnO}_3$, the evolution with x of the character of the conduction electrons is controlled by three transitions: (1) from static to dynamic cooperative Jahn-Teller deformations of the MnO_6 octahedra occupied by high-spin Mn(III) ions, (2) from localized to itinerant behavior of the conduction electrons, and (3) from ordered to disordered arrangements of the charge carriers [1,2]. We report measurements of the transport properties under different hydrostatic pressures that were taken on two single-crystal samples, $x = 0.12$ and 0.15 ; they demonstrate a transition from nonmetallic to metallic behavior in a narrow temperature interval $T_{\text{co}} < T < T_c$ between a charge-ordered state for $T < T_{\text{co}}$ and a paramagnetic state for $T > T_c$. We interpret the transport data below T_c with a mobile-cluster model.

The perovskite system $\text{La}_{1-x}\text{Sr}_x\text{MnO}_3$ contains high-spin Mn atoms in octahedral sites of a MnO_3 array having $(180^\circ - \phi)$ Mn-O-Mn bonds. Bending of the Mn-O-Mn bonds from 180° by a cooperative rotation of the MnO_6 octahedra reduces the mismatch between the Mn-O and the mean La,Sr-O equilibrium bond lengths; rotations about a cubic [110] axis reduce the space-group symmetry to orthorhombic, about a [111] axis to rhombohedral. A cooperative, static Jahn-Teller deformation reduces the axial ratio of the orthorhombic phase from $c/a > \sqrt{2}$ to $c/a < \sqrt{2}$; we distinguish, in Fig. 1, O orthorhombic structures (with $c/a > \sqrt{2}$) from O' orthorhombic structures (with $c/a < \sqrt{2}$). The rhombohedral structure R is not compatible with a static, cooperative Jahn-Teller deformation, but dynamic deformations may occur in the O phase.

The threefold-degenerate π -bonding $3d$ orbitals at the Mn atoms are half-filled and, for all x , form localized t_2^3 configurations with a spin $S = \frac{3}{2}$; the $t_2^3\text{-O:}2p_\pi\text{-}t_2^3$ superexchange interactions are isotropic and antiferromagnetic. A single e electron per Mn(III) ion occupies the twofold-degenerate σ -bonding orbitals; a strong Hund's intra-atomic-exchange coupling to the t_2^3 electron spin removes the intra-atomic spin degeneracy, and the e -orbital degeneracy is removed by a local Jahn-Teller deformation

of the Mn(III) sites to tetragonal or orthorhombic symmetry. Cooperativity among the local deformations, which may be static or dynamic, greatly reduces the cost in elastic energy of the deformations.

In a perovskite MnO_3 array, Jahn-Teller deformations are achieved by displacements of the oxygen atoms from one near neighbor toward the other to create asymmetric $(180^\circ - \phi)$ Mn...O-Mn bonds. The resulting $e^1\text{-O:}2p_\sigma\text{-}e^0$ superexchange interactions are ferromagnetic and stronger than the antiferromagnetic $t_2^3\text{-O:}2p_\pi\text{-}t_2^3$, but they are anisotropic. In LaMnO_3 , for example, static Jahn-Teller deformations order the $e^1\text{-O:}2p_\sigma\text{-}e^0$ interactions into (001) planes to give an O' orthorhombic structure with $c/a < \sqrt{2}$; consequently, the (001) planes are ferromagnetically coupled, but these planes are coupled antiferromagnetically along the c axis, where the $t_2^3\text{-O:}2p_\pi\text{-}t_2^3$ superexchange interactions are dominant to give type-A antiferromagnetic order [1,2]. A Dzialoshinskii antisymmetric superexchange component cants a few

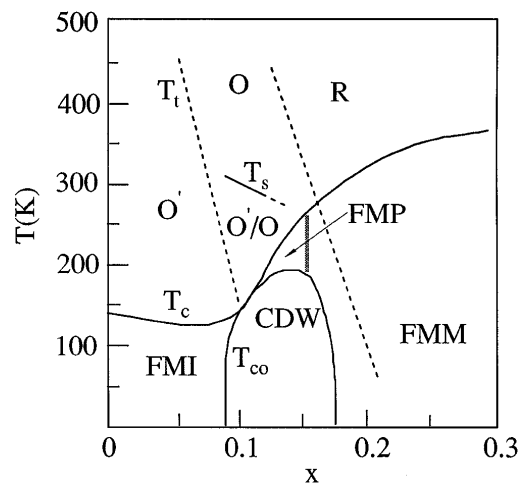


FIG. 1. Modified phase diagram for $\text{La}_{1-x}\text{Sr}_x\text{MnO}_3$. The vertical line is the estimated boundary of transition from the FMP to FMM state. FMI (ferromagnetic insulator), FMP (ferromagnetic polaron), FMM (ferromagnetic metal).

degrees the spins on the two sublattices to give a weak ferromagnetism [3].

With increasing x in the system $\text{La}_{1-x}\text{Sr}_x\text{MnO}_3$, a change from O' to O orthorhombic occurs near $x = 0.1$ at a temperature $T_t > T_c$ (see Fig. 1). The Mn(IV) ions introduced by Sr substitution create ferromagnetic double-exchange interactions via fast electron transfer within Mn(III)-O-Mn(IV) clusters and suppress the static Jahn-Teller deformation. In the interval $0.1 < x < 0.3$, dynamic deformations remain at the Mn(III) centers and the magnetic order changes from antiferromagnetic (with a weak ferromagnetic component) to ferromagnetic; the long-range magnetic-ordering temperature T_c increases by over 200 K [4]. The temperature dependence of the resistance above T_c is semiconductive; below T_c it changes from semiconductive to metallic near $x = 0.11$ [4]; but in the range $0.11 \leq x < 0.15$ a jump in $\rho(T)$ at T_{co} marks the onset of semiconductive behavior below T_{co} (see Fig. 1). Yamada *et al.* [5] have identified a charge-ordered phase below T_{co} . Charge ordering in the O orthorhombic phase represents a segregation below T_{co} into hole-rich (001) planes containing dynamic Jahn-Teller deformations alternating with Mn(III)O₂ planes containing a static Jahn-Teller ordering of the oxygen displacements as in the (001) planes of LaMnO_3 . In this Letter, we present evidence for a polaronic state in the range $T_{co} < T < T_c$; an extensive literature has provided evidence for polaronic conduction above T_c , e.g., [6,7]. We have chosen for study the single-crystal samples $x = 0.12$ and $x = 0.15$ that were used to reveal the charge-ordered phase with neutron diffraction and had been characterized with chemical analysis, ambient-pressure resistivity, and magnetic-susceptibility measurements [4].

The two single crystals, grown by the floating-zone method [4], were cut into rectangular bars ($1.5 \times 1 \times 0.5 \text{ mm}^3$) with a diamond saw. Resistivity measurements under high pressure were carried out with a four-probe method. Thin Cu wires were pressed onto the sample surface with pieces of indium foil. Details of our thermoelectric-power (TEP) measurements under high pressure have been described elsewhere [8]. The cooling rate was controlled at 0.2 K/min in order to maintain hydrostatic pressure.

Figures 2 and 3, show respectively, the resistivity vs temperature under several pressures for $x = 0.12$ and $x = 0.15$. The ambient-pressure curves for the two samples are identical with the independent earlier results [4], except for the jump in resistivity near $T_s \approx 278 \text{ K}$ found with the $x = 0.12$ sample. (A similar weak feature was found near 290 K with $x = 0.10$, Fig. 2 of Ref. [4].) This jump, which exhibits a thermal hysteresis (see inset of Fig. 2), cannot be attributed to the O - R transition at T_t since $T_t \approx 500 \text{ K}$ for $x = 0.12$. Under hydrostatic pressure, the temperature interval over which the jump occurs becomes larger, but the transition temperature does not change. The neutron data [5] identified a first-order transition at $T_{co} = 148 \text{ K}$ and a second-order transition at

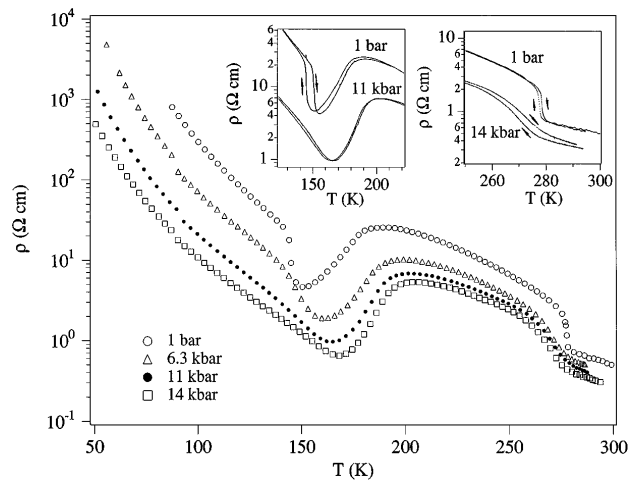


FIG. 2. Resistivity $\rho(T)$ under several hydrostatic pressures for $\text{La}_{0.88}\text{Sr}_{0.12}\text{MnO}_3$. Insets show thermal hysteresis at T_{co} and T_s .

$T_{co} = 192 \text{ K}$, respectively, for the $x = 0.10$ and $x = 0.15$ samples. We can therefore identify the minimum in the resistivity vs temperature curves with T_{co} ; the thermal hysteresis (inset of Fig. 2) is consistent with a first-order transition at T_{co} in the $x = 0.12$ sample.

According to the neutron-diffraction data [5], the holes in the Mn(IV)/Mn(III) redox couple are ordered into every other (001) MnO_2 plane below T_{co} . A cooperative Jahn-Teller deformation orders ferromagnetic $e^1\text{-O:}2p_\sigma\text{-}e^0$ interactions within the Mn(III)O₂ sheets just as in LaMnO_3 ; the Mn(IV) ions are ordered on one-quarter of the Mn sites in the alternate (001) planes. However, a dynamic segregation into hole-rich and hole-poor regions below a $T_s > T_{co}$ would remain undetected by a diffraction experiment, and we believe that such a dynamic phase segregation is occurring below $T_s \approx 278 \text{ K}$ in the $x = 0.12$ sample. In the $x = 0.15$ sample, on the other hand, it appears that $T_s \approx T_c$.

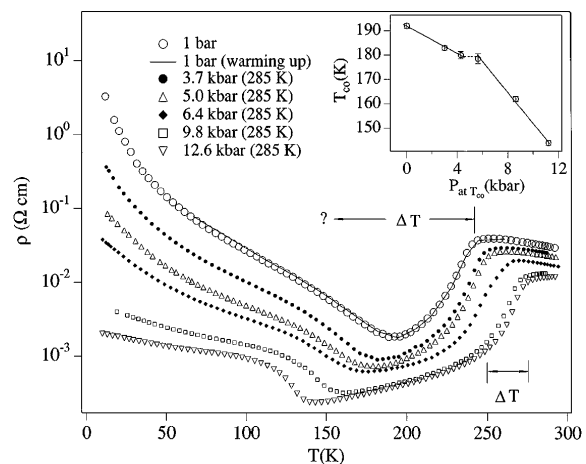


FIG. 3. Resistivity $\rho(T)$ under several hydrostatic pressures for $\text{La}_{0.85}\text{Sr}_{0.15}\text{MnO}_3$. Inset shows T_{co} vs P at T_{co} . Large ΔT below T_c for $P < 5 \text{ kbar}$ is to be distinguished from small ΔT for $P > 6 \text{ kbar}$.

From Fig. 2, it is apparent that, in the $x = 0.12$ sample, high pressure both raises T_{co} and converts the transition at T_{co} from first order to second order; the thermal hysteresis is barely resolvable at 11 kbar. On the other hand, T_{co} decreases under pressure for the $x = 0.15$ sample. In the phase diagram of Fig. 1, T_{co} vs x is a maximum within the range $0.12 < x < 0.15$, so pressure influences T_{co} in the same way as an increase in x .

The maximum in the resistivity vs temperature curves in Figs. 2 and 3 occurs near the Curie temperature T_c as determined by neutron diffraction [5]. Pressure increases T_c for both samples, which again parallels the effect of increasing x . The dramatic change with temperature in the resistivity in a ΔT below T_c is typical of that found [9,10] in the $\text{Ln}_{0.7}\text{A}_{0.3}\text{MnO}_3$ compositions (Ln = rare earth, A = alkaline earth) having a $T_c < 250$ K; it occurs in an interval $\Delta T = (T_c - T_{co})$ in the $x = 0.12$ samples and in the $x = 0.15$ samples under pressures $P < 5$ kbar. Under a pressure $P > 6$ kbar, on the other hand, the $x = 0.15$ crystal shows a sharply reduced ΔT and a range of temperature $T_{co} < T < T_c - \Delta T$ in which the resistivity falls less steeply with decreasing temperature. Figure 3 shows that this temperature range increases with pressure $P > 6.4$ kbar and, see inset, that there is a discontinuity in dT_{co}/dP in the pressure range $5 < P < 6.4$ kbar. In order to determine whether this discontinuity and the change in ΔT mark a transition from polaronic to metallic behavior below T_c , we investigated the thermoelectric power (TEP) under pressure.

The temperature dependence of the TEP, $\alpha(T)$, taken under several pressures is shown in Figs. 4 and 5 for $x = 0.12$ and $x = 0.15$, respectively. For $x = 0.12$, the $\alpha(T) > 0$ curve shows, on cooling, a marked increase setting in below $T_s = 278$ K, a sharp decrease occurring in the interval $T_{co} < T < T_c$, and an abrupt increase on crossing T_{co} that is followed by a continued, more gradual increase to a maximum value at lower temperatures. Hydrostatic pressure increases the rise in $\alpha(T)$ below T_s and shifts the changes associated with T_{co} and T_c to higher temperatures with the same pressure dependence as that determined from Fig. 2. The pressure dependence of $\alpha(300$ K) passes through a maximum, which is unusual.

In the $x = 0.15$ sample, the resistivity data of Fig. 3 show a T_c that increases sensitively with pressure, a T_{co} that decreases with increasing pressure. The arrows in Fig. 5 mark the T_{co} obtained from Fig. 3. With no visible T_s far removed from room temperature, $\alpha(300$ K) shows a monotonic decrease with increasing pressure that is quite steep. On cooling, the $\alpha(T)$ curves of Fig. 5 drop abruptly at T_c , but they increase on cooling through T_{co} as in the $x = 0.12$ crystal only for pressures $P \leq 4.1$ kbar. For $P \leq 4.1$ kbar, $\alpha(T)$ is pressure dependent in the interval $T_{co} < T < T_c$. For $P \geq 6.7$ kbar, $\alpha(T)$ decreases on cooling through T_{co} and the $\alpha(T)$ curves are pressure independent in the range $T_{co} < T < T_c$. Thus the data of Fig. 5 clearly confirm a change in the character of the conduction electrons of the $x = 0.15$ sample between

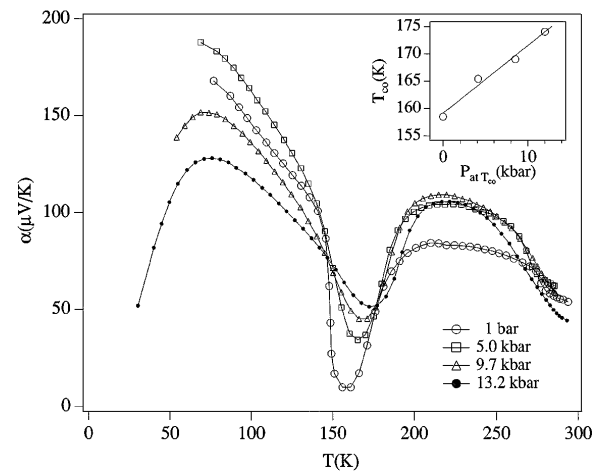


FIG. 4. Thermoelectric power $\alpha(T)$ under several hydrostatic pressures for $\text{La}_{0.88}\text{Sr}_{0.12}\text{MnO}_3$. Inset shows T_{co} vs P at T_{co} .

5 and 6 kbar as was made evident in Fig. 3. At lower pressures, the TEP is sensitive to the charge-carrier density, as is made evident by the abrupt increase of TEP on cooling through T_{co} . Therefore the TEP of the low-pressure phase appears to be dominated by the statistical contribution as in a polaron conductor, whereas for $P > 6$ kbar it is dominated by the transport contribution as in a metal.

Zener [11] proposed the first model to make a connection between ferromagnetic order and an enhanced electrical conductivity with a metalliclike temperature dependence. His double-exchange model consisted of clusters of two manganese atoms in which fast, real charge transfer occurs within the equilibrium reaction $\text{Mn(III)-O-Mn(IV)} = \text{Mn(IV)-O-Mn(III)}$; he postulated that these two-manganese clusters would move diffusively with no motional enthalpy below T_c , so their mobility $\mu_c = eD_0/kT$ would give a linear variation of $\rho = (pe\mu_c)^{-1}$ vs T . A second double-exchange model was proposed by de Gennes [12], who assumed that the charge carriers are itinerant below T_c . Although the de Gennes model

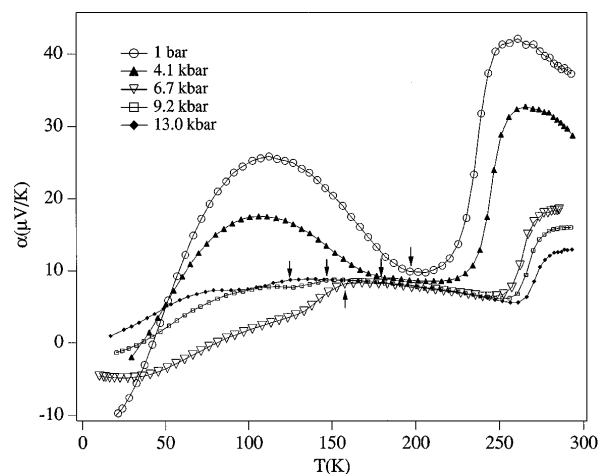


FIG. 5. Thermoelectric power $\alpha(T)$ under several hydrostatic pressures for $\text{La}_{0.85}\text{Sr}_{0.15}\text{MnO}_3$.

has been widely accepted, it appears to be applicable only for samples with $T_c > 250$ K; in these samples, the resistivity drops abruptly on cooling through T_c and varies nearly linearly with T from a few degrees below T_c [13]. The TEP also drops abruptly to a small, temperature-dependent value on cooling through T_c [10,14]. However, the de Gennes model is quite misleading in the range of carrier concentrations p and/or geometrical tolerance factor t where T_c changes sensitively with p and t , e.g., $0.10 < x < 0.15$ in Fig. 1. The changes with p and/or t in Mn-O-Mn bond angle, which is related to the width of the conduction band, are too small for the de Gennes model to account for a change of over 200 K in the Curie temperature T_c , and the temperature dependence of the resistivity in the range $T_{co} < T < T_c$ does not appear to signal itinerant-electron conduction at ambient pressure in the $x = 0.12$ and $x = 0.15$ samples. In all the manganese oxides having $60 < T_c < 250$ K, the resistivity change below T_c is not typical of a metal-nonmetal transition. On the other hand, the resistivity does not behave below T_c as predicted from the Zener model; rather it increases more sharply than exponentially over a considerable temperature range as T_c is approached from below [10]. Moreover, the pressure dependence of T_c is anomalously high for a conventional order-disorder magnetic transition [15]. What is missing from these models is a strong electron interaction with cooperative, dynamic oxygen-atom displacements; and the observation [16] of a giant isotope effect on T_c with the exchange of ^{18}O for ^{16}O has demonstrated that such an interaction must be introduced. We shall therefore refer to this unusual electronic state below T_c as a polaronic state.

If our conclusion is valid, i.e., if $\alpha(T)$ for a polaronic state is dominated by the statistical contribution, then the TEP is given by

$$\alpha \approx -(k/e) \ln[(1-c)/c] \quad (1)$$

for a magnetically ordered state. In samples $\text{Ln}_{0.7}\text{Ca}_{0.3}\text{MnO}_3$ having $60 < T_c < 250$ K, charge ordering is avoided and therefore $\alpha(T)$ drops to a small, temperature-independent value below T_c , whereas $\rho(T)$ decreases monotonically with $T < T_c$ over a wide temperature range [10]. According to Eq. (1), an $\alpha \approx 0$ requires that the effective fraction c of manganese sites that are occupied by a charge carrier is $c \approx 0.5$. This condition would be satisfied for $x = 0.33$ if the charge carrier consisted of Mn(III)-O-Mn(IV)-O-Mn(III) three-manganese clusters in which the hole was alternately at one of the two Mn(III) ions and was made mobile by a dynamic Jahn-Teller coupling to the oxygen vibrations between manganese atoms. Identification of three-manganese clusters at 18 K in $\text{La}_{1-x}\text{Sr}_x\text{MnO}_3$ has recently been made by Louca *et al.* [17]. The nonadiabatic polaron containing

three Mn centers and an internal vibration between two degenerate orbital configurations represents a vibronic state that should be distinguished from a conventional polaronic state.

In summary, the data of Fig. 2–5 lead to the following four principal conclusions: (1) Where T_c increases sharply with x in the system $\text{La}_{1-x}\text{Sr}_x\text{MnO}_3$, i.e., for $0.1 < x \leq 0.15$, the electrons are not itinerant below T_c as assumed by de Gennes. (2) We have identified in the $x = 0.15$ crystal a transition from the polaronic (vibronic) to an itinerant-electron state in the pressure range $5 < P < 6$ kbar. (3) In the polaronic regime below T_c , we can account for an $\alpha \approx 0$ in the $\text{Ln}_{0.7}\text{Ca}_{0.3}\text{MnO}_3$ samples with mobile three-manganese clusters instead of the two-manganese clusters postulated by Zener [11]. (4) We have suggested that a first-order phase change found in the $x = 0.12$ crystal at $T_s = 278$ K $> T_c$ may represent a dynamic phase segregation into hole-rich and hole-poor electronic phases above the transition to a static charge-ordered phase below $T_{co} < T_c$.

The authors (J.S.Z. and J.B.G.) thank the Robert A. Welch Foundation, Houston, TX, and NSF for financial support.

-
- [1] E.O. Wollan and W.C. Koehler, *Phys. Rev.* **100**, 545 (1955).
 - [2] J.B. Goodenough, *Phys. Rev.* **100**, 564 (1955).
 - [3] J.B. Goodenough and J.M. Longo, *Landolt-Börnstein Tabellen*, edited by K.H. Hellwege, New Series III/4a, (Springer-Verlag, Berlin, 1970), p. 126.
 - [4] A. Urushibara, Y. Moritomo, T. Arima, A. Asamitsu, G. Kido, and Y. Tokura, *Phys. Rev. B* **51**, 14 103 (1995).
 - [5] Y. Yamada, O. Hino, S. Nolido, R. Kanao, T. Inami, and S. Katano, *Phys. Rev. Lett.* **77**, 904 (1996).
 - [6] S.J.L. Billinge, R.G. DiFrancesco, G.H. Kwei, J.J. Neumeier, and J.D. Thompson, *Phys. Rev. Lett.* **77**, 715 (1996).
 - [7] J.M. De Teresa *et al.*, *Nature (London)* **386**, 256 (1997).
 - [8] J.-S. Zhou and J.B. Goodenough, *Phys. Rev. B* **54**, 13 393 (1996).
 - [9] H. Y. Hwang, S.-W. Cheong, P.G. Radaelli, M. Marezio, and B. Batlogg, *Phys. Rev. Lett.* **75**, 914 (1995).
 - [10] J.-S. Zhou, W. Archibald, and J.B. Goodenough, *Nature (London)* **381**, 770 (1996).
 - [11] C. Zener, *Phys. Rev.* **82**, 403 (1951).
 - [12] P.-G. de Gennes, *Phys. Rev.* **118**, 141 (1960).
 - [13] J.J. Neumeier, M.F. Hundley, J.D. Thompson, and R.H. Heffner, *Phys. Rev. B* **52**, R7006 (1995).
 - [14] J. Hejtmanek *et al.*, *Phys. Rev. B* **54**, 11 947 (1996).
 - [15] Y. Moritomo, A. Asamitsu, and Y. Tokura, *Phys. Rev. B* **51**, R16491 (1995).
 - [16] G.-M. Zhao, K. Conder, H. Keller, and K.A. Müller, *Nature (London)* **381**, 676 (1996).
 - [17] D. Louca, T. Egami, E.L. Brosha, M. Röder, and A.R. Bishop, *Phys. Rev. B* (to be published).